New bis(triazinyl) pyridines for selective extraction of americium(III)

Michael J. Hudson,*[a] Carole E. Boucher,[a] Damien Braekers,[b] Jean F. Desreux,[b] Michael G. B. Drew,[a] Mark R. St J. Foreman,[a] Laurence M. Harwood,[a] Clément Hill,[c] Charles Madic,[c] Frank Marken[d] and Tristan G. A. Youngs[a]

Received (in Montpellier, France) 4th October 2005, Accepted 21st June 2006
First published as an Advance Article on the web 12th July 2006
DOI: 10.1039/b514108g

New hydrophobic, tridentate nitrogen heterocyclic reagents (BATPs) such as 2,6-bis (5,5,8,8-tetramethyl-5,6,7,8-tetrahydrobenzo[1,2,4]triazin-3-yl) pyridine (**1**) and 2,6-bis (9,9,10,10-tetramethyl-9,10-dihydro-1,2,4-triaza-anthrane-3-yl) pyridine (**2**) have been studied. **1** is resistant to hydrolysis in 3 M nitric acid, whereas **2** is resistant to both acid hydrolysis and radiolysis. The molecules are able to give significantly enhanced separations of americium(III) from an excess of europium(III) in nitric acid. Typically, for **1** $D_{Am} = 500$ and $SF_{Am/Eu} = 5000$ compared with $D_{Am} = 30$ and $SF_{Am/Eu} = 400$ with the reference molecule 2,6-bis (isopropyl[1,2,4]triazin-3-yl) pyridine (**7**). In order to increase the stability of **1** and **2**, the labile α-benzylic hydrogens that are present in **7** have been replaced by alkyl groups. Three molecules of **1** are able to enclose completely the coordination sphere of the M(III) in the crystal structure of $[Y(\mathbf{1})_3][Y(NO_3)_5] \cdot NO_3 \cdot 2.5H_2O$.

Introduction

The transplutonium elements (and their decay products) are responsible for the majority of the long lasting radiotoxicity in waste from the PUREX reprocessing of used nuclear fuel.[1] After their removal from used fuels the transuranium elements can be either used in radioactive sources or transmuted by neutron bombardment to short lived radionuclides[2–4] either in conventional critical nuclear reactors or in sub-critical accelerator driven systems.[5,6] One of the principal obstacles to a process for the removal of americium and curium from the waste is the fact that a selective metal-binding reagent with the required properties of radiation stability, chemical stability, and solubility has yet to be identified. Recently, the 1,2,4-triazin-3-yl oligopyridines (BTPs, shown in Fig. 1) have been identified as metal extractants, which have the ability to separate actinides(III) [An(III)] and lanthanides(III) [Ln(III)] from nitric acid[7] but the resistances of the BTPs to radiolysis and chemical hydrolysis are insufficient for the development of an industrial process.[8] The selective complexation of An(III) as opposed to Ln(III) is an important problem for fundamental as well as applied chemistry.[9,10] For the treatment of spent fuels, lanthanides are able to absorb neutrons, which may be used to transmute long-lived radionuclides of americium(III) or curium(III) to short-lived ones. The evaluation of new metal-binding agents for the actinides and lanthanides provides a means of probing the comparative chemistries of the An(III) and Ln(III).[11] For instance the variation of the coordination of oxygen and nitrogen donors to the different lanthanides has been the subject of recent studies.[12,13]

Fig. 1 shows molecules **1**, **2** and the 2,6-bis([1,2,4]triazin-3-yl) pyridines (**3** to **7**) for the SANEX process, in which minor An(III) are separated selectively from Ln(III).[14] The reference molecule **7** is an example of a BTP-type molecule in which there are two triazine rings and one central pyridine ring; this compound has been considered as a stable version of **6** which has been tested using macroscopic amounts of americium and curium.[8] These BTP molecules can bind as tridentate ligands to metal cations. Crystal structures of Sm(III), Tm(III) and Yb(III) with **6** show that the coordination spheres of the cations are filled completely by the three molecules of **6** in complexes of the type $[M(III)(\mathbf{6})_3] \cdot [NO_3]_3$.[15] In solution, the BTP molecules, including those with larger alkyl groups attached to the triazine rings, are able to form such complexes.[16,17] These observations are important since nitrate and water molecules are often bound to the metal cations when less potent extraction agents such as terpyridines are used.[18] The nitrate and water molecules are potentially able to interchange rapidly so that multiple terpy-containing species are formed, which are of different composition and overall charges. For clearly defined and efficient separations there is a need to reduce the number of species that are involved in the partitioning—preferably to have a single species.[19]Therefore, polydentate nitrogen heterocycles that completely fill the coordination sphere of the metal are promising reagents. If a metal binding agent (extractant) is to be used to process a radioactive liquor the extractant must be able to resist both radiolytic degradation and the effects of nitrogen oxo-acids. The reference molecule **7** is more resistant to hydrolysis by 0.5 M nitric acid, which is the acidity of the feed solution for the SANEX process, than **6**, but **7** is subject to extensive and rapid hydrolysis in more concentrated nitric acid (3 M), and is extensively (>80%) radiolysed by doses such as 100 kGy of

[a] *School of Chemistry, University of Reading, Box 224, Whiteknights, Reading, Berkshire, UK RG6 6AD. E-mail: m.j.hudson@reading.ac.uk*
[b] *University of Liège, Coordination and Radiochemistry, Sart Tilman B16, Liège, B-4000, Belgium*
[c] *Commissariat à l'Energie Atomique, Valrho (Marcoule) B.P. 17171-30207, Bagnols-sur Cèze Cedex, France*
[d] *Department of Chemistry, University of Bath, Bath, UK BA2 7AY*

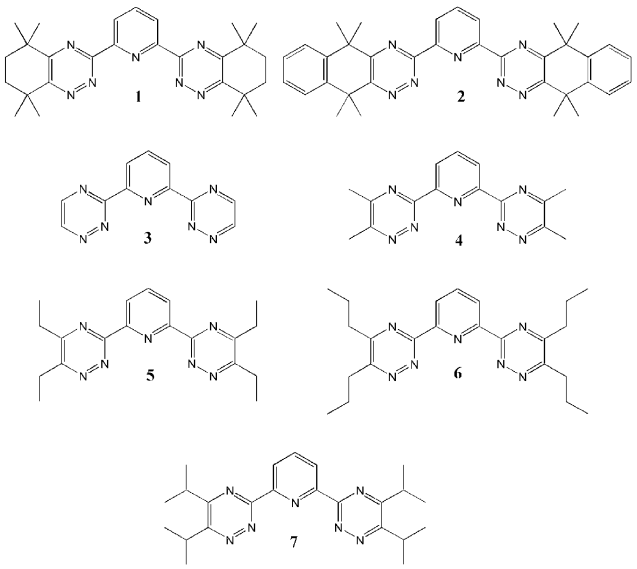

Fig. 1 2,6-Bis(5,5,8,8-tetramethyl-5,6,7,8-tetrahydrobenzo[1,2,4]triazine-3-yl) pyridine (**1**) (all compounds are drawn in the *cis*,*cis* conformation); 2,6-bis(9,9,10,10-tetramethyl-9,10-dihydro-1,2,4-triazaanthrane-3-yl) pyridine (**2**); 2,6-bis(1,2,4-triazine-3-yl) pyridine (**3**); 2,6-bis(5,6-dimethyl[1,2,4]triazine-3-yl) pyridine (**4**); 2,6-bis(5,6-diethyl[1,2,4]triazine-3-yl) pyridine (**5**); 2,6-bis(5,6-dipropyl[1,2,4]triazine-3-yl) pyridine (**6**); 2,6-bis(5,6-diisopropyl[1,2,4]triazine-3-yl) pyridine (**7**).

γ-radiation. Consequently, attempts have been made in this study to design alternative BTP-type molecules, which are more resistant to hydrolysis or radiolysis, but which are able to give quantitative separations of An(III) from Ln(III). The new molecules are designated BATPs (A = annulated) since, although they retain many of the features of BTPs they have additional annulated rings. In the case of **1** this ring is a saturated cyclohexyl group but in **2** there is an additional aromatic ring. This distinction between the two types of annulated rings is important because it will be shown that the aromatic ring provides an extra means of granting resistance to radiolysis.

Through careful design of an organic compound or by appropriate selection of conditions under which it is exposed, the rate of degradation due to the action of ionising radiation can be reduced. For instance in the same way that the addition of a free radical initiator is unable to alter the thermodynamics of the polymerisation of styrene, gamma irradiation is unable to influence the thermodynamics of the reaction of potassium hydroxide, isopropanol and a polychlorobiphenyl. But the rates of reaction can be increased by the use, respectively of a free radical initiator and gamma irradiation.[20–22] Both the free radical initiator and gamma irradiation increase the rates of reaction by introducing the reactive species which initiate chain reactions. In both the free radical polymerisation and the radiolytic dechlorination the presence of substances which intercept the reactive intermediates (respectively oxygen and nitrobenzene) thus reduce the rate of reaction. An alternative to inhibiting free radical polymerisation by the addition of an inhibitor is to choose a monomer which is less able to polymerise. For instance in the copolymerisation of styrene with vinyl acetate and methyl acrylate it has been shown that the free radical formed by the reaction of styrene is better able to react with methyl acrylate than vinyl acetate. As it is clearly possible by molecular design to alter the susceptibility of an alkene to form a polymer, it was reasoned that by the correct design the degradation rates associated with irradiation and reactive chemical species could be reduced.

The degradation of an organic compound induced by radiation may be caused either by the chemical attack by a radiogenic reactive intermediate (indirect radiolysis), or by energy transferred to the molecule by the radiation (direct radiolysis). The key difference between the direct and indirect radiolysis is that in an indirect process degradation can continue to occur after the irradiation is terminated. A hypothetical example of indirect radiolytic damage would be a chloride facilitated corrosion of a steel object in a radiolytic polychlorobiphenyl dehalogenation plant, in this example the radiolysis of the polychlorobiphenyls would create chloride anions which could at a later time come into contact with the water and the steel surface.

The resistance to hydrolysis by nitrogen oxo-acids is required because aqueous chemical processing of used nuclear fuel is normally performed in nitric acid. In addition to nitric acid, nitrous acid is often present in these aqueous mixtures, nitrite is formed by the irradiation of aqueous nitric acid[23] and in some nuclear reprocessing plants nitrogen oxides are used as process chemicals. Nitrous acid can readily decompose to form nitrogen dioxide, and it has been shown that nitrogen dioxide is able to degrade organic compounds.[24] In addition to the radiogenic reactive species; other reactive species formed from other process chemicals are likely to be present. As it has been shown that nitrogen oxides can attack alkylarenes through the abstraction of benzylic hydrogen atoms,[24] so a series of extractants, which are devoid of benzylic hydrogen atoms were prepared.

Chemical attack upon the α-benzylic hydrogens has been shown to be responsible for much of the degradation of **7** by nitrogen oxo-acids. In order to prevent the chemical degradation which is mediated by nitrite ions or nitrogen oxides all the α-benzylic hydrogens have been replaced by alkyl groups attached to annulated rings. It is known that the nature of the solvent (diluent) has a strong influence on the radiation stability of organic compounds,[25] for instance benzene may either sensitise or protect another hydrocarbon by energy transfer.[26] It has also been shown that the presence of aromatic hydrocarbons greatly reduces the radiochemical yield of the decomposition product dibutyl hydrogen phosphate from tributylphosphate.[27] In this case, it is thought that the aromatic π-systems are able to adsorb some of the energy from the radiation, which otherwise leads to the radiolysis of tributylphosphate. Clearly, the aromatic groups are protecting the tributylphosphate through an intermolecular process. However, it has never been shown before that it is possible to design molecules for the separation of Am(III) and Eu(III), which have an annulated, aromatic π-system that is able to absorb and dissipate some of the energy from the radiation that could cause degradation. In this study, therefore, it has

been attempted to reduce the effects of direct radiation by incorporating the extra annulated rings in **2** compared with **1** or **7**.

Consequently, attempts have been made in this study to design alternative BTP-type molecules, which are more resistant to hydrolysis or radiolysis, but which are able to give quantitative separations of An(III) from Ln(III). The new molecules are designated BATPs (A = annulated) since, although they retain many of the features of BTPs, they have additional annulated rings. In the case of **1** this ring is a saturated cyclohexyl group but in **2** there is an additional aromatic ring.

Experimental

^{1}H, ^{13}C–{^{1}H} and ^{13}C NMR spectra were recorded using either a Bruker AMX400 or an Avance DPX250 instrument, unless stated otherwise all samples for NMR experiments were dissolved in deuterochloroform. Chemical shifts are reported in parts per million downfield from tetramethylsilane. The lanthanum titration was performed using a method analogous to that reported for the titration of dimethyl *hemi*-BTP with yttrium nitrate.[10] Relaxivity titrations were performed at 25 °C and 20 MHz with a Bruker Minispec. The longitudinal relaxation times T_1 were measured by the inversion recovery pulse sequence. Anhydrous lanthanide perchlorates were prepared as reported previously.[28] ***Caution**: lanthanide perchlorates are potentially explosive when brought into contact with organic materials. Only use small quantities of these metal salts.* All materials and solutions required for the relaxivity titrations were handled under argon in a glove box. All organic reagents were purchased from Acros or Aldrich, while inorganic reagents were obtained from either BDH or Aldrich. **1** and **2** are indicative of a new range of BATP molecules, which have been synthesised using the method of Case in which the reaction of 2,6-dicarbonitrile pyridine with hydrazine led to pyridine-2,6-dicarboxamide hydrazone.[29] This hydrazone was condensed with either 3,3,6,6-tetramethylcyclohexane-1,2-dione[30] or 1,1,4,4-tetramethyl-3,4-dihydro-1*H*-naphthalen-1,2-dione[31] to form the desired BATP derivatives.[29] 6,6′-Bis(5,6-dimethyl-1,2,4-triazin-3-yl)-2,2′-bipyridine (**9**) was prepared using a method analogous to that used to form 6,6′-bis(5,6-diethyl-1,2,4-triazin-3-yl)-2,2′-bipyridine.[32]

Synthesis

Synthesis of 1. 2,6-Pyridine dicarboxamide dihydrazone (598 mg, 3.1 mmol) and 3,3,6,6-tetramethylcyclohexane-1,2-dione (1.04 g, 6.2 mmol) were refluxed in absolute ethanol (60 ml) for 3 h. Evaporation of the solvent *in vacuo* led to a yellow orange crystalline solid (2.24 g, 100%). A small amount was recrystallised from diethyl ether to yield orange rhombohedra. Mp 144–148 °C. Found: C, 70.3; H, 7.5; N, 21.1%; $C_{27}H_{35}N_7$ requires C, 70.9; H, 7.7; N, 21.4%. δ_H 8.6 (2H, d, ^{3}J = 7.8 Hz), 8.0 (1H, t, ^{3}J = 7.8 Hz), 1.8 (8H, m), 1.4 (12H, s) and 1.4 (12H, s) ppm. δ_H 163.2, 162.2, 159.9, 153.0, 136.9, 123.9, 36.4, 35.5, 32.7, 32.4, 28.7 and 28.2 ppm. MS (CI+) (MH+) 458, 428, 294 and 121 *m*/*z*. Molecular ion found at 458.3021 ($^{12}C_{27}{}^{1}H_{35}{}^{14}N_7$ requires 458.3032, error of 2.4 ppm).

Synthesis of 2. Pyridine 2,6-dicarboxamide hydrazone (784 mg, 4.05 mmol) and 1,1′,4,4′-tetramethyl-2,3-naphthalenedione (1.75 g, 8.1 mmol) were refluxed in ethanol (15 ml) for 2.5 h. Evaporation of the solvent led to a crystalline orange solid (2.25 g). Mp 140–142 °C. Found: C, 75.2; H, 6.2; N, 17.8%; $C_{35}H_{35}N_7$ requires C, 75.9, H; 6.4; N, 17.7%. δ_H 8.8 (2H, d, ^{3}J = 7.8 Hz), 8.2 (1H, t, ^{3}J = 7.8 Hz), 7.6 (4H, m), 7.4 (4H, m), 1.9 (12H, s) and 1.89 (12H, s) ppm. δ_C 160.5, 159.7, 153.0, 139.0, 139.0, 137.1, 126.2, 125.5, 124.2, 39.0, 39.0, 31.5 and 31.5 ppm. MS (CI+) 554 (MH+), 525 and 169 *m*/*z*. Molecular ion found at 554.3017 ($^{12}C_{35}{}^{1}H_{36}{}^{14}N_7$ requires 554.3032, error of 2.7 ppm).

Synthesis of 9. A mixture of powdered 2,2′-bipyridine 6,6′-dicarboxamide hydrazone (1.88 g. 6.96 mmol), triethylamine (10 ml), butane-2,3-dione (20 ml) and tetrahydrofuran (700 ml) was heated. Before the temperature had reached boiling point a golden yellow solution was obtained, from this solution a solid rapidly precipitated. After boiling this cloudy mixture under reflux for 6 h, the product was collected by filtration (paper filter) of the hot reaction mixture. After washing with boiling hot THF (100 ml) the solid (2.12 g. 82%) was dried in air and then *in vacuo*. Found: C, 65.2; H, 5.0; N, 29.9%; $C_{20}H_{18}N_8$ requires C, 64.9; H, 4.9; N, 30.2%.

The synthesis of yttrium tris{2,6-bis(5,5,8,8-tetramethyl-5,6,7,8-tetrahydrobenzo[1,2,4]triazin-3-yl) pyridine} pentanitratoyttrium nitrate. 2,6-Bis(5,5,8,8-tetramethyl-5,6,7,8-tetrahydrobenzo[1,2,4]triazin-3-yl) pyridine (2.09.3 mg. 457.7 μmol) was dissolved in dichloromethane (2 ml). To this solution was added a solution of yttrium nitrate hexahydrate (121 mg. 316 μmol) in acetonitrile (4 ml). After combining the solutions the mixture was concentrated by slow evaporation, before crystals were harvested. These crystals (82 mg, 43 μmol, 28%) were washed with cold acetonitrile and diethyl ether before being allowed to dry. Found: C, 49.0; H, 5.4; N, 19.5%; $Y_2C_{81}H_{105}N_{27}O_{18}$ requires C, 50.6; H, 5.5; N, 19.7%.

The synthesis of nickel(II) bis{2,6-bis(5,5,8,8-tetramethyl-5,6,7,8-tetrahydrobenzo[1,2,4]triazin-3-yl) pyridine} perchlorate. [Ni(1)$_2$]·2ClO$_4$. To a solution of **1** (200 mg. 437 mmol) in deoxygenated ethanol (12 ml) was added nickel(II) chloride hexahydrate (52 mg. 219 mmol). Within seconds a red coloration was observed, this mixture was heated under reflux with the exclusion of oxygen for 4 hours before being allowed to cool. After the removal of the ethanol *in vacuo*, the brown residue was dissolved in deoxygenated water. By the addition of a deoxygenated sodium perchlorate solution the product was precipitated; the mixture was allowed to stand overnight to allow the precipitation process to complete. From this point onwards no effort was made to exclude atmospheric oxygen from the reaction mixture. The product was collected by filtration, and was washed with water, cold ethanol and cold diethyl ether before being allowed to dry in air (241 mg, 92%). Found C, 53.9; H, 5.8; N, 16.4%; $[Ni(C_{27}H_{35}N_7)_2]\cdot 2ClO_4\cdot 1\frac{1}{2}H_2O$ requires C, 54.1; H, 6.1; N, 16.4%.

Solvent extraction

The organic solutions were prepared by dissolving either **1** or **2** in a solvent (diluent) with or without a phase modifier.

Table 1 Typical conditions for solvent extraction studies[a]

Mixing time/min	5	15	30	45	60
$A(^{152}Eu)_{ini}$/kBq L^{-1}	7850				
$A(^{152}Eu)_{eq,aq}$/kBq L^{-1}	7640	7190	6965	6535	6030
$A(^{152}Eu)_{eq,org}$/kBq L^{-1}	380	790	1250	1515	1870
D_{Eu}	5.0×10^{-2}	1.1×10^{-1}	1.8×10^{-1}	2.3×10^{-1}	3.1×10^{-1}
$A(^{241}Am)_{ini}$/kBq L^{-1}	10350				
$A(^{241}Am)_{eq,aq}$/kBq L^{-1}	720	20	20	20	20
$A(^{241}Am)_{eq,org}$/kBq L^{-1}	10170	11150	10570	9775	10050
D_{Am}	14	558	529	489	503
$SF_{Am/Eu}$	284	5074	294	2108	1620
$[HNO_3]_{ini}$/mol L^{-1}	0.50				
$[HNO_3]_{eq}$/mol L^{-1}	0.49				

[a] A = radioactivity; D = distribution ratio; SF = separation factor; ini = initial; eq = equilibrium.

N,*N*′-Dimethyl-*N*,*N*′-dioctyl-2-(2-hexoxyethyl) malondiamide (DMDOHEMA) was used as a phase modifier with the novel BATP molecules. These solutions were pre-equilibrated with nitric acid solutions of the same concentration as was used to form the radioactive test solutions. The aqueous solutions were prepared by spiking aqueous nitric acid with stock solutions of ^{152}Eu and ^{241}Am. The radioisotopes were obtained and used as previously described.[10,33] Table 1 shows typical conditions for the solvent extraction studies using **1** and **2**. For the organic phase $[\mathbf{1}]_{initial}$ = 0.01 mol L^{-1} in the mixture: *n*-octanol/$[DMDOHEMA]_{ini}$ = 0.50 mol L^{-1}, pre-equilibrated with nitric acid ($[HNO_3]_{ini}$ = 0.5 mol L^{-1}). For the aqueous phase which simulated a MO_x spent fuel solution $[HNO_3]_{ini}$ = 0.5 mol L^{-1} + [Ln(III)] = 8.8×10^{-3} mol L^{-1} + ^{241}Am and ^{152}Eu at trace level. $V_{org} = V_{aq}$ = 700 μL, temperature = 25 °C. No precipitate was formed even after three weeks of contact.

Computational chemistry

Quantum mechanics calculations were carried out using density functional theory using the ADF program[34] at the TZP level. Calculations were carried out in the gas phase and then in solvent using the COSMO method that provides a conductor-like screening method for solvation. COSMO is a dielectric model in which the solute molecule is embedded in a molecular-shaped cavity surrounded by a dielectric medium with a given dielectric constant.[35]

Crystallography

Crystallographic data are given in Table 2.† X-Ray diffraction data for the two crystals were collected with Mo-Kα radiation using the MAR research image plate system. The crystals were positioned at 70 mm from the image plate. Ninety-five frames were measured at 2° intervals with a counting time of 2 min or more where appropriate. Data analysis was carried out with the XDS program.[36] The structures were solved using direct methods with the SHELX86 program.[37] Non-hydrogen atoms were refined with anisotropic thermal parameters apart from several light atoms at the extremities of the ligands in the Y complex which when refined anisotropically gave unrealistic ellipsoids. The hydrogen atoms bonded to carbon were included in geometric positions and given thermal parameters equivalent to 1.2 times those of the atom to which they were attached. In the metal complexes, the hydrogen atoms bonded to water molecules could not be located. An empirical absorption correction was carried out on the metal complex using the DIFABS program.[38] The structures were refined on F^2 until convergence using SHELXL.[39]

Electrochemistry

All electrochemical experiments were conducted using a computer-controlled Autolab potentiostat (PGSTAT 30, Ecochemie, Netherlands). Solution state electrochemical experiments were performed in deoxygenated acetonitrile in the presence of tetraethylammonium perchlorate (0.25 M). Tetraethylammonium perchlorate was obtained by the addition of perchloric acid to aqueous tetraethylammonium bromide, and was recrystallised twice from water before being dried *in vacuo* to a constant mass. ***Caution:*** *treat all organic perchlorates as potential explosives; tetraethylammonium perchlorate is a known explosive*.[40] The working electrode was a 3 mm glassy carbon disk purchased from Bioanalytical Systems, a silver wire was used as a quasi-reference electrode and the counter-

Table 2 Crystallographic details of the crystal structures

	1	$[Y\mathbf{1}_3]\cdot[Y(NO_3)_5]\cdot NO_3$
Empirical formula	$C_{27}H_{35}N_7$	$C_{81}H_{115}N_{27}O_{20.5}Y_2$
Formula weight	457.62	1972.82
System, space group	Monoclinic, $P2_1/a$	Monoclinic, $C2/c$
a/Å	14.496(15)	34.86(4)
b/Å	11.318(12)	14.790(17)
c/Å	16.793(18)	40.64(4)
β/°	102.40(1)	97.11(1)
Volume/Å^3	2691	20789
Z, ρ (calculated) M gm^{-3}	4, 1.130	8, 1.261
Absorption coefficient mm^{-1}	0.070	1.185
Reflections collected	7099	56610
Unique data	4021	17907
Restraints	0	0
Parameters	316	1173
Final R indices $[I > 2\sigma(I)]R_1$, wR_2	0.0874, 0.2086	0.0940, 0.2028
R indices (all data)	0.1778, 0.2422	0.2879, 0.2678
Largest diff. peak and hole e Å^{-3}	0.361, −0.228	0.428, −0.341

† CCDC reference numbers 206177 and 232470. For crystallographic data in CIF or other electronic format see DOI: 10.1039/b514108g

electrode was a platinum wire. Solution state potentials were measured using the ferrocene/ferrocenium couple (ferrocene added as an internal standard) and are expressed relative to the ferrocene/ferrocenium couple. Cyclic voltammetry was performed using a staircase waveform with a step size typically of 0.1 mV. The formal potentials for reversible events were calculated as the midpoint of potentials of the anodic and cathodic current peaks. The formal potentials are expressed relative to the ferrocene/ferrocenium couple. All experiments were conducted under an argon (BOC) atmosphere and at a temperature of 22 ± 2 °C.

Results and discussion

The crystal structure of **1** is shown in Fig. 2, together with the numbering scheme of the nitrogen atoms. This structure is defined as the *trans*,*trans* (*tt*) conformation as characterised by the N(11)–C–C–N(21) and N(31)–C–C–N(21) torsion angles. This *tt* conformation has been shown by quantum mechanics calculations (see later) to have a lower energy than the *cis*,*cis* (*cc*) conformation that is to be found in all the metal complexes with BATP (and BTP) molecules. It seems probable that this *tt* conformation is the dominant conformer in neutral solution as well as in the solid state. Consequently, metal complexation of the unprotonated form with both **1** and **2** involves a change in conformation, as is the case with the other BTPs. In the crystal structure of the unbound molecule **1**, rather surprisingly, the two outer rings are not coplanar with the central ring making angles of 29.5 and 29.6°, respectively. No obvious reason for these large angles is apparent, although packing effects are the likely cause. The *tt* conformation adopted by the unprotonated form contrasts with the protonated form which adopts the *cc* conformation (see later).

Solvent extraction

Fig. 3 compares the kinetics of extraction of **1**, **2** and **7** in the presence of *N*,*N*′-dimethyl-*N*,*N*′-dioctyl-2-ethoxymalondiamide (**8**) (0.5 mmol L^{-1}) in *n*-octanol, for an aqueous solution simulating an MO_x spent fuel $[HNO_3]_{initial}$ = 0.5 mol L^{-1} and Ln(III) at 8.8 mmol L^{-1} with ^{241}Am and ^{152}Eu at trace levels. However, the respective initial concentration of **1**, **2** and **7** were 0.01, 0.02 and 0.01 mmol L^{-1}. For **1**, the time for 50% extraction of Am(III) is approximately 5 min and over 90% is extracted after 30 min. The corresponding rate of extraction of Eu(III) is much slower and the time for 50% extraction is much greater than 90 min. Both **1** and **2** have slower rates of extraction than **7**, for which the time for 50% extraction is less than 1 min. However with **1**, after 15 min, the values for $[D_{Am(III)}]$ is significantly greater than that for the reference molecule **7**. At the same time the $D_{Eu(III)}$ value with **1** is only 0.1. Therefore, the separation factor (*SF*) between Am(III) and Eu(III) is *ca.* 5600, which is an order of magnitude higher than the corresponding value with the reference molecule **7**, which has previously been regarded as a rather effective partitioning reagent. Such a high value for the separation factor between Am(III) and Eu(III) has never been obtained before at such a high concentration of nitric acid. It is also potentially useful for recovering traces of Am(III) and other similar radionuclides. With **2**, the $[SF_{Am/Eu}]$ values are also greater than that of the reference molecule **7** although the $[D_{Am(III)}]$ values are lower. For example, after 15 min, $[SF_{Am/Eu}]$ was 560, which is much higher than that obtained with the reference molecule **7**.

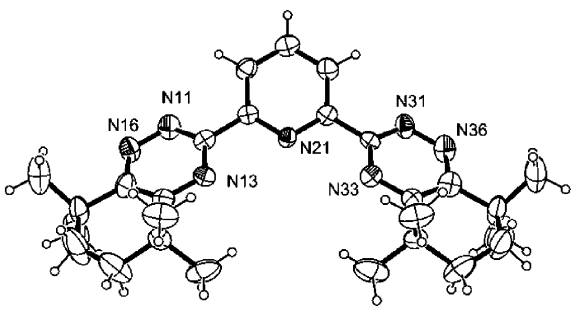

Fig. 2 The crystal structure of **1** in the *trans*,*trans* conformation.

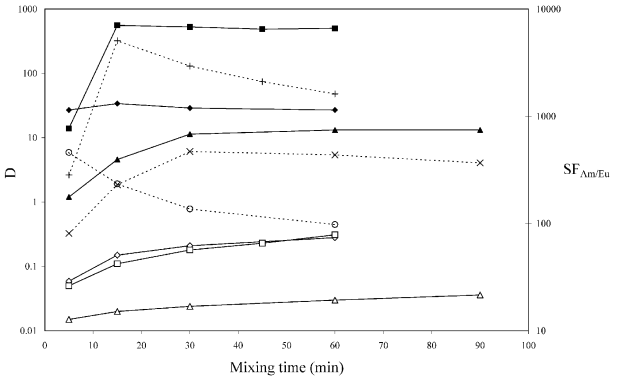

Fig. 3 Extraction of Am(III) and Eu(III) from nitric acid (0.5 M) at 25 °C. Key ■ D_{Am} with **1** and **8**; □ D_{Eu} with **1** and **8**; + $SF_{Am/Eu}$ with **1** and **8**; ▲ D_{Am} with **2** and **8**; △ D_{Eu} with **2** and **8**; × $SF_{Am/Eu}$ with **2** and **8**; ◆ D_{Am} with **7**; ◇ D_{Eu} with **7**; ○ $SF_{Am/Eu}$ with **7**.

Both of the BATP reagents **1** and **2** are poorer extractants in the absence of the phase modifier. For **1** alone in *n*-octanol, D_{Am} = 0.6 after 15 min, which corresponds to 38% Am(III) extraction, and D_{Am} = 3.9 after 60 min (79% extraction). Fig. 4 shows the effect of **8** on the rate and extraction efficiency of **2** in *n*-octanol. The BATP **2** has slower kinetics of extraction than **1** since it is a larger molecule.

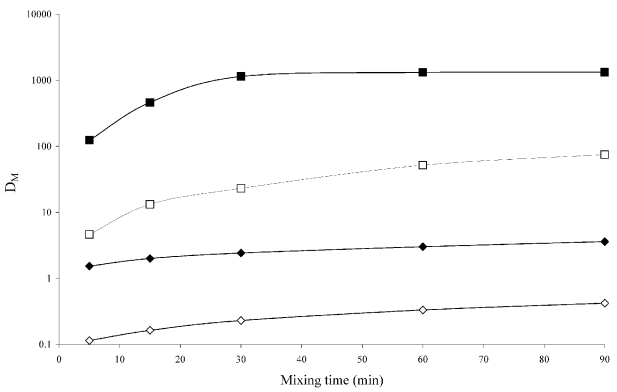

Fig. 4 Extraction of Am(III) and Eu(III) from nitric acid (0.5 M) at 25 °C by **2**, in the presence and absence of the malonamide **8**. Key ■ D_{Am} with **8** (0.5 mol L^{-1}); □ D_{Eu} with **8** (0.5 mol L^{-1}); ◆ D_{Am} with **8** absent; ◇ D_{Eu} with **8** absent.

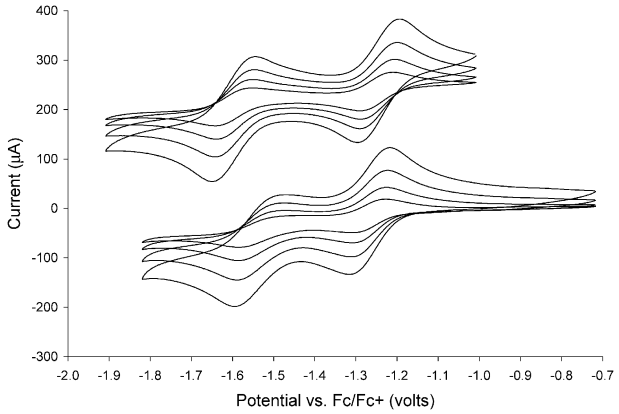

Fig. 5 Cyclic voltammograms of $[Ni(\mathbf{1})_2]^{2+}$ (top) and $[Ni(\mathbf{5})_2]^{2+}$ (bottom), showing the formation of $[Ni(\mathbf{1})_2]^0$ and $[Ni(\mathbf{5})_2]^0$. For each compound scans recorded at 200, 100, 50 and 25 mV s^{-1} are shown. The peak currents are controlled by the diffusion (mass transport).

Resistance to chemical degradation and radiolysis

Molecules **1** and **2** were not hydrolysed by boiling nitric acid (3 M) over 24 h, whereas the reference molecule **7** was extensively decomposed. With respect to radiolysis, after an integrated dose of 100 kGy there was more than 80% degradation of the reference molecule **7** and a similar extent of degradation of **1** in *n*-octanol, but only 15% degradation of **1** in the mixture *n*-octanol–nitrobenzene. This degradation is thought to come from direct radiolysis. However, there was no degradation of **2** after an integrated dose of 100 kGy in *n*-octanol, which is known to be able to produce aggressive reagents such as free radicals groups on irradiation. Thus, it appears that the additional annulated ring in **2** does add significant extra resistance to radiolysis. This means that there is clear evidence that molecules such as **2** can have improved resistance to both direct and indirect radiolysis by the incorporation of an annulated aromatic π-system.

It has been shown that the solvated electron is responsible for many degradation processes associated with irradiation,[20,41] and that the transition metal complexes of the BTP ligands have a rich electrochemistry which is complicated by the instability of some of the reduced metal complexes.[42] It was reasoned that, if the side groups in **1** are able to isolate a reactive central core of a complex from its surroundings, then these side groups will be able to isolate the central core of the complex from an incoming reactive species. As a partly reversible Ni(I)/(0) redox event had been observed for $[Ni(\mathbf{5})_2]^+$ in acetonitrile at −1.54 V, the nickel complex of **1** was prepared. As shown in Fig. 5, it was found that for $[Ni(\mathbf{1})_2]^+$ the metal centred Ni(I)/(0) redox couple at −1.60 V was fully reversible, suggesting that the side groups in **1** inhibit the non-electroactive chemical reaction coupled to the electrochemical reduction of the Ni(I) complex. It was found that at a more reducing potential (−2.15 V) a ligand centred multi-electron reduction of $[Ni(\mathbf{1})_2]^0$ occurred; while this event is not fully reversible under the same conditions the corresponding event for $[Ni(\mathbf{5})_2]^0$ at −2.03 V is almost totally irreversible, suggesting again that the side groups in **1** are more able than those on **5** to isolate the core of the complex from its surroundings. Reversible one electron oxidations and reductions were observed for $[Ni(\mathbf{1})_2]^{2+}$ at 1.02 and −1.25 V, respectively, the analogous one electron oxidation reaction of $[Ni(\mathbf{5})_2]^{2+}$ occurred at 1.19 V.

Species that are present in the organic phase

In order to better understand the process of extraction it was important to establish how many molecules of **1** are able to coordinate to a trivalent lanthanide centre. We wished to know if the metal centre could accommodate three molecules of **1** in an analogous way to that in which three bis(5,6-dialkyltriazin-3-yl) pyridine molecules can fit around a lanthanide centre.[43,16,17] It was found that a 2:3 mixture of yttrium nitrate and **1** in acetonitrile formed crystals of $[Y(\mathbf{1})_3]\cdot[Y(NO_3)_5]\cdot NO_3$. The structure consists of discrete $[Y(\mathbf{1})_3]$ trications, $[Y(NO_3)_5]$ dianions and nitrate anions, and five water molecules, each with 50% occupancy. The cation is shown in Fig. 6 and the geometry is such that the metal cation is bound to three tridentate ligands with Y–N distances ranging from 2.426(8) to 2.522(8) Å. It is probable that Am(III) and Eu(III) also form such 1:3 complexes. The tridentate molecules are approximately planar with the outer rings intersecting the plane of the inner ring in each ligand by less than 10°. It is noteworthy, particularly in the context of separation, that the anion also contains the metal. In previous crystallographic studies of lanthanide nitrate complexes with the non-annular BTPs, both nitrates and anionic nitrato lanthanide complexes have been present as counterions.[15] While it is possible to extract anionic complexes of trivalent metals by an ion pair extraction mechanism using a quaternary ammonium salt (such as Aliquat 336, *N*,*N*,*N*-trimethyl-*N*-octylammonium chloride) from aqueous nitrate media,[44] this

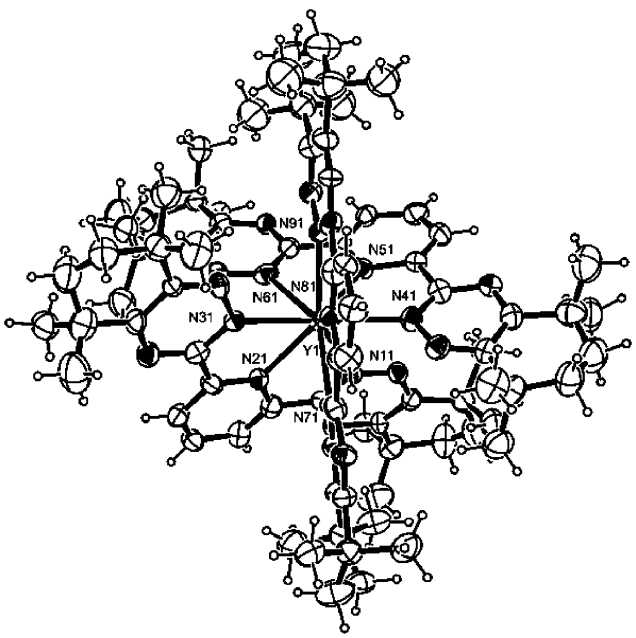

Fig. 6 The crystal structure of the $[Y(\mathbf{1})_3]$ trication. Bond lengths from Y are to N(11) 2.511(7), N(21) 2.470(9), N(31) 2.451(8), N(41) 2.476(9), N(51) 2.461(8), N(61) 2.522(8), N(71) 2.493(7), N(81) 2.426(8) and N(91) 2.507 Å.

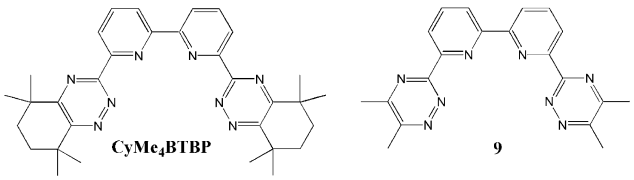

Fig. 7 The structures of **CyMe$_4$BTBP** and 6,6′-bis(5,6-dimethyl-1,2,4-triazin-3-yl)-2,2′-bipyridine (**9**).

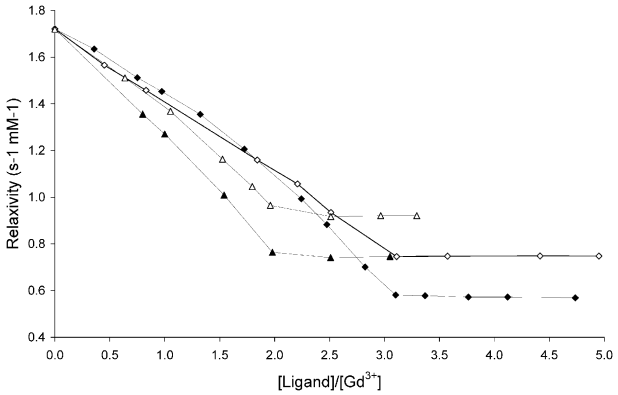

Fig. 8 The relaxation titrations of anhydrous gadolinium(III) perchlorate with **1**, **4**, **9** and **CyMe$_4$BTBP**. Key ◆ **1**; ◇ **4**; ▲ **CyMe$_4$BTBP**; △ **9**.

extraction mechanism is surpassed by the extraction of nitric acid from the aqueous phase.[45] As nitric acid is extracted by a combination of octanol and the diamide, we expect that this ion pair extraction mechanism will be suppressed, so only nitrate and possibly pertechnetate anions will be present as the counterions within an americium loaded organic phase found in a solvent extraction experiment if the total metal content of the organic phase remains low. However if the cation concentration in the organic phase was exceptionally high, for instance if a large amount of an interfering metal formed organic soluble cationic complexes with the extractant, then the extraction of anionic nitrato metal complexes would become more likely.

Information on the solution structures can be gained from a detailed NMR analysis of the lanthanide complexes. The Gd(III) ion is known to cause a strong acceleration of the proton relaxation rate of solvent molecules because of its high magnetic moment and the spherical distribution of its unpaired electronic spins.[46] This property has been exploited to develop contrast agents for magnetic resonance imaging and is relatively well understood because of the recent work based on the Solomon–Bloembergen equations.[47] A relaxation titration of anhydrous gadolinium(III) perchlorate with **1** in anhydrous acetonitrile is presented in Fig. 8 in the form of the dependence of relaxivity [relaxation rate $1/T_1$ per mmol of Gd(III)] *vs.* the ligand/metal concentration ratio. The binding of **1** displaces solvent molecules from the coordination sphere of the gadolinium ions; these solvent molecules then relax more slowly when in the bulk of the solution. Consequently, the relaxivity decreases until a plateau is reached when a complex is fully formed.[48] The bipyridine derivatives **CyMe$_4$BTBP**[32] and 6,6′-bis(5,6-dimethyl-1,2,4-triazin-3-yl)-2,2′-bipyridine (**9**) (shown in Fig. 7) obviously form bis-complexes while the pyridine derivatives **1** and **4** form tris-complexes in anhydrous acetonitrile.

The sudden breaks in the relaxivity titrations indicate that these complexes are quite stable. The observed stoichiometries are in keeping with the number of coordinating groups featured by the ligands. Three BTP molecules such as **1** or **4** are needed to completely encapsulate Gd(III) as these ligands have only three nitrogen atoms available for bonding. With four donor groups, only two BTBP ligands such as **CyMe$_4$BTBP** or **9** are required to complete the coordination sphere of Gd(III). It should be noted here that the relaxivities do not decrease linearly with the ligand/metal ratios. Perfectly linear relationships are expected if only bis- or tris-complexes are formed for the BTPs and BTBPs, respectively. Intermediate mono- and bis-complexes are also present in solution as demonstrated below by an analysis of the NMR spectra of diamagnetic species. Each intermediate has its own relaxivity properties and the relaxivity *vs.* ligand/metal ratio is no longer linear. Possibly some of these complexes are not partially solvated by acetonitrile. The lowest relaxivity plateau is obtained for **1** and it can be assumed that the coordination sphere of Gd(III) is complete with 9 nitrogen donor groups and bulky tetramethylcyclohexyl substituents. The relaxivities observed for high ligand/metal ratios would then be entirely due to acetonitrile molecules near the complex. Although further removed from the paramagnetic ions, these molecules still contribute to the total relaxivity as already observed in water. A higher relaxivity plateau is observed for the complex with the bipyridine analogue **CyMe$_4$BTBP** and it can be assumed that this complex is better solvated. The total relaxivity decrease for **1** is 1.15 s^{-1} $mmol^{-1}$ and corresponds to the removal of 8 or 9 acetonitrile molecules.[49] The exclusion of one acetonitrile molecule thus corresponds to a relaxivity decrease of approximately 0.13–0.14 s^{-1} $mmol^{-1}$. The relaxivity difference between the plateaus of **1** and **CyMe$_4$BTBP** is 0.17 s^{-1} $mmol^{-1}$; one could suggest that the Gd(III) bis-complex with **CyMe$_4$BTBP** remains solvated by one acetonitrile molecule. Replacing the tetramethylcyclohexyl substituents of BTP and BTBP by methyl groups leads to relaxivity plateaus that are systematically higher. It thus seems that the bulkiness of the substituents is an important factor that limits the solvation. However this line of reasoning is only valid if a comparison between two complexes is limited to species that tumble in solution at the same rate. The Solomon–Bloembergen equations indeed show that the relaxivity depends on the correlation factors for the rotation, the solvent exchange and the electronic relaxation. The smallest of these factors dominates the relaxivity. For small complexes like the one being considered here, relaxivity depends entirely on rotation which is the fastest process. Relaxivity increases with the size of the Gd(III) complexes as rotation becomes slower. One would thus expect that the relaxivity plateau would be higher for the complexes with the largest ligands such as **1** and **CyMe$_4$BTBP** since they rotate more slowly. It is the opposite that is observed and it can be concluded that solvation is indeed limited by bulky substituents. A similar effect has been observed by mass spectrometry and is quite unusual.

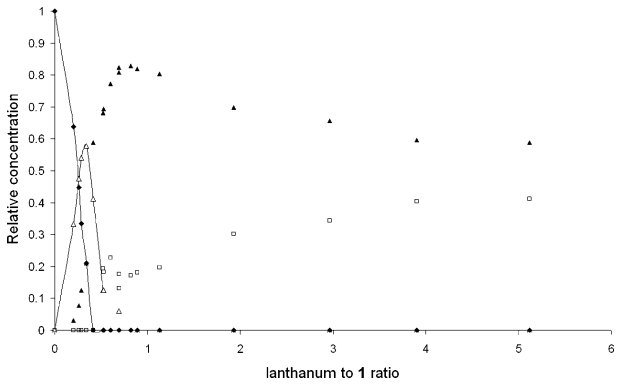

Fig. 9 NMR titration of **1** with lanthanum nitrate in acetonitrile. Key ◆ Free ligand **1**; △ $\{La(\mathbf{1})_3\}_n$; ▲$\{La(\mathbf{1})_2\}_n$; □ $\{La(\mathbf{1})\}_n$.

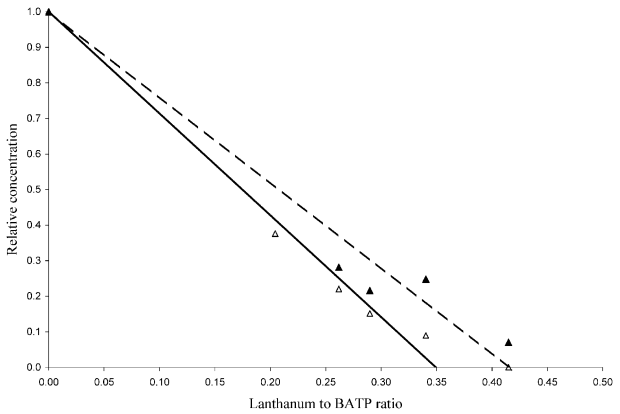

Fig. 10 Relative concentrations of the free ligand in both the presence and absence of the diamide (*N*,*N*′-dimethyl-*N*,*N*′-dicyclohexylmalondiamide). Key △ free ligand in the absence of the diamide; ▲ free ligand in the presence of the diamide.

It is reasonable to assume a high distribution ratio is obtained if a chelating extractant completely encapsulates a metal ion to form a lipophilic entity. This could be achieved by forming a *homoleptic* complex of a lipophilic ligand. If a hydrophilic ligand, such as water or nitrate, was to be attached to the metal then it is conceivable that the resulting *heteroleptic* complex will be less lipophilic because the solvent accessible surface will now include a larger hydrophilic region. These relaxivity experiments have demonstrated that the side groups bonded to the triazine rings of **1** have a great ability to isolate the central core of the complex in a nine coordinate tris-BTP metal complex. Further relaxivity experiments with these BTP and BTBP[32] ligands are currently being undertaken.

Titration of lanthanum nitrate with **1** (monitored by ^{1}H NMR spectroscopy) confirms the formation of a 1:3 complex such as the $[La(\mathbf{1})_3]$ trication. With respect to La–**1** complexes in acetonitrile, the ratio **1**/La may be 1, 2 or 3 depending on the **1**:La ratio originally in solution, Fig. 9. There is evidence to suggest that the free ligand and the $[La(\mathbf{1})_3]$ trication; the $[La(\mathbf{1})_3]$ and $[La(\mathbf{1})_2]$ trications; $[La(\mathbf{1})_2]$ and $[La(\mathbf{1})]$ trications are in equilibrium, but the $[La(\mathbf{1})]$ trication is not present when there is free ligand **1** in solution. It was observed in 1:1 methanol–water that the bis(5,6-dialkyltriazin-3-yl) pyridines with larger alkyl groups (**6** and **7**) were better able to form $[Eu(L)_3]$ tricationic complexes than was Me_4BTP (**4**).[16,17] It was even noted for **6** and **7** that 1:2 mixtures of europium nitrate and the organic ligands contained the $[Eu(L)_3]$ tricationic complexes. It was reasoned that the hydrophobic nature of the larger side groups favoured the formation of these 1:3 complexes. It is evident from Fig. 9 that, even when the concentration of lanthanum nitrate exceeds that of **1**, the 1:2 complex ($[La(\mathbf{1})_2]^{3+}$) is present in the mixture. While this NMR study was performed in acetonitrile rather than the water–methanol mixture it is reasonable to suggest that the lipophilic side groups attached to **1** may well favour the formation of the 1:2 complex over the 1:1 complex.

One explanation for the acceleration of the americium extraction, caused by the addition of the malonamide to the diluent, into octanol is that the malonamide forms a complex with the americium which is more able to cross the aqueous–organic interface than either the extractant (**1**) or the americium complexes found in a solution of americium(III) in aqueous nitric acid. This malondiamide complex of americium would then react with **1** to form free malondiamide and a complex such as the $[Am(\mathbf{1})_3]$ trication. To investigate the relative binding abilities of **1** and the malonamide a series of further NMR experiments were undertaken. In these experiments an excess of malonamide was added to a mixture of lanthanum nitrate and **1** in acetonitrile. The aromatic regions of the NMR spectra obtained from the malonamide-containing samples were analogous to the spectra recorded using the malonamide-free samples. It is thought that the chemical shifts of the complexes $\{La(\mathbf{1})_n\}$ (n = 1, 2 or 3) are not changed greatly by the addition of the malonamide. From the NMR spectra it is clear that similar complexes (formed between lanthanum and **1**) are formed no matter whether the malonamide is present or absent.

It was found that the malonamide was able to partly inhibit the formation of the 3:1 complex, suggesting that **1** and the malonamide compete for the lanthanum centres. In the absence of any malondiamide the initial slope for the free ligand in Fig. 9 suggests that 2.9 molecules of **1** are able to bind to each lanthanum. However, when an excess of *N*,*N*′-dimethyl-*N*,*N*′-dicyclohexylmalondiamide is added to the solution of $[La(\mathbf{1})_3]$ trication then the initial slope of the graph of the relative concentration of the free ligand **1** with respect to the **1**/La ratio was reduced to 2.4, as shown in Fig. 10. The fact that even in the presence of an excess of malonamide the $[La(\mathbf{1})_3]$ and $[La(\mathbf{1})_2]$ tricationic complexes can exist suggests that the conversion of a malonamide complex of lanthanum into a lanthanum complex of **1** is feasible, suggesting in turn that the phase transfer of americium by a malonamide is a possible explanation for the change in the rate of extraction.

Computational chemistry

Conformations adopted by the BATP and BTP molecules. Quantum mechanics calculations were carried out, using density functional theory using the ADF program at the TZP level, on **1**, **2**, and **3** in order to study the electronic properties and conformational preferences for the neutral and mono- or diprotonated BATP molecules, Fig. 11. Calculations

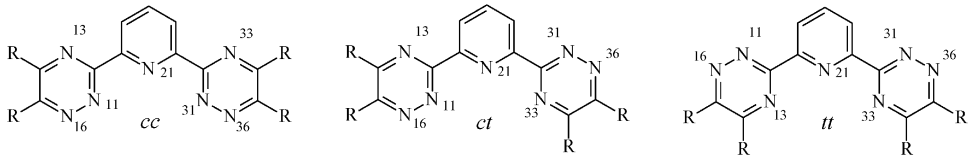

Fig. 11 Conformations of **3**.

were carried out in the gas phase and then in solvent using the COSMO method that provides a conductor-like screening method for solvation. COSMO is a dielectric model in which the solute molecule is embedded in a molecular-shaped cavity surrounded by a dielectric medium with a given dielectric constant. The three possible conformations of **1**, **2** and **3** were considered, and their structures were converged with dielectric constants ranging from 1 to 80. The results are compared in Table 3, together with values for terpyridine.

For each of the unbound or free (unprotonated) ligands, in the gas phase, the *tt* conformation is significantly lower in energy than the *cc* form, with the *ct* form intermediate between the two values (Table 3). The energy for the interconversion between the *cc* and *ct* conformers at the TZP level can be calculated as the difference in energy between the *tt* form and the intermediate (transition-state) geometry with the outer rings perpendicular to the central pyridine ring. This energy difference is very similar in all structures and of the order of 35–38 kJ mol^{-1}, though slightly larger for **2**. However, each of these values is significantly less than that calculated for terpyridine (67.92 kJ mol^{-1}) for which rotation involves clashes of *ortho*-hydrogen atoms in adjacent rings. Despite the energy barrier of 35–38 kJ mol^{-1} between the *tt* and the *cc* conformers, it seems likely that there is a facile interconversion from the *tt* conformer to the *cc* conformer, which may bind to an M(III) cation, Fig. 11. This interconversion probably does not have a detrimental effect on the separation process from neutral aqueous solutions.

It can be assumed that the aqueous layer in the separation process has a high dielectric constant and therefore that the energy difference between the conformations is very low. Indeed for all the ligands the difference between the *cc* and *tt* conformations decreases rapidly with dielectric constant and at 80, the *cc* conformation becomes the most favourable. This can be compared with the results for terpy which show a similar decrease in energy difference but the *tt* remains the lowest energy difference. Here the charge distribution is not so important as the repulsion between bridgehead hydrogen atoms.

Preferential sites for protonation

Monoprotonation. It is possible that in the extraction process protonation occurs since the extractions are done from acidic aqueous media. In the protonated forms it is the *cc* conformer, which is required for binding to metals, that is present. In the molecules of **3** the three different conformations (*cc*, *ct* or *tt*), each with four different nitrogen atoms that can be protonated, and all combinations were considered to give rise to twelve different structures, which were energy minimised using the ADF program. The structures with the lowest energies are described in Table 4—the energies are relative to the structure with the lowest energy. As has been found for other terdentate ligands, the most favourable gas phase structure is *cis*,*cis* with the central N(21) protonated, which gives rise to two intramolecular hydrogen bonds to adjacent nitrogen atoms.

Protonation in any other position in any of the three conformers results in either a repulsive interaction between hydrogen atoms, causing rotation of the outer rings and loss of some degree of aromaticity and relative stability, or a less-strong H-bonding interaction. All other structures have energies in excess of 29.12 kJ mol^{-1} greater than the minimum energy structure, this energy difference being found for N(11) in the *cc* conformation. Indeed, the three lowest energy structures occur when the central pyridine nitrogen N(21) is protonated. Less predictable is the change in the energy ordering of the conformers. Whereas the order $tt < ct < cc$ is observed for the neutral species, when the central pyridine nitrogen is protonated, the order is reversed to $cc < tt < ct$ so that the lowest energy conformer is that found in metal complexation. This result indicates that a stronger hydrogen bond can be formed from N(21) to N(11) than can be formed to N(13). Protonation of the molecules holds them in the *cc* conformer required for binding to the metal cation. Therefore, the extraction mechanism involves exchange of the proton in the protonated *cc* conformer by an M(III) cation.

The results using various dielectrics show that the energy differences between the *cc* and *tt* protonated structures decrease with increasing dielectric constant although surprisingly

Table 3 The relative energies of the *ct* and *cc* conformations compared to the *tt* conformation of the molecules **1**, **2**, and **3** (kJ mol^{-1}) after geometry optimisation with various dielectric constants (ε_r) at the TZP level

Conformation	*cc*				*ct*			
ε_r	1	5	10	80	1	5	10	80
Molecule								
1	14.67	5.12	1.92	−1.52	2.80	1.39	2.55	4.46
2	22.39	8.92	3.47	−0.73	6.59	5.80	4.33	2.36
3	17.10	6.95	2.99	−1.28	10.36	8.08	6.03	2.94
Terpy	59.88	24.29	15.89	7.66	25.47	12.87	9.49	6.82

Table 4 The structures with the lowest relative energies for $[\mathbf{3}\text{-H}]^+$

(ε_r)		Energy difference/kJ mol^{-1}				Protonation energy/kJ mol^{-1}			
Conformation	Protonation site	1	5	10	80	1	5	10	80
cc	N(21)	0.00	0.00	0.00	0.00	192.88	30.95	14.89	−0.89
tt	N(21)	4.04	1.42	0.05	−0.05	207.00	39.32	17.94	−2.23
ct	N(21)	4.75	5.67	5.33	5.88	197.35	35.49	17.18	0.78

the difference is maintained between the *cc* and *ct*. The protonation energies are also included, showing that these decrease from *ca.* 200 kJ mol^{-1} to *ca.* 0 kJ mol^{-1} as the dielectric increases from 1 to 80; so in aqueous solution, protonation is favoured.

Diprotonation. All likely combinations of conformations for the diprotonated **1**, **2** and **3** molecules (*cc*, *ct* and *tt*) and protonation sites were studied and the four structures with the lowest relative energies are described in Table 5.

Results for $[\mathbf{1}\text{-2H}]^{2+}$ show that the lowest energy arrangements do not involve the protonation of N(21), as has been found for the monoprotonated compound, because there is subsequently no low energy site for the second proton. In contrast, the lowest-energy arrangement sees protonation in both outer rings so as to form intramolecular hydrogen bonds to the central nitrogen atom. However the lowest energy conformation does vary between the ligands. For **3**, with no substituents, there are three structures with similar energies within 1 kJ mol^{-1} but in **1** and **2** the preferences change with one structure having the lowest energy by 13.1 kJ mol^{-1} for **1** and 18.1 kJ mol^{-1} for **2**. It seems likely that, to proceed from the monoprotonated LH^+ to the diprotonated LH_2^+, the hydrogen on N(21) will migrate to the adjacent N(11) with the second proton being added to either N(31) or N(36). The variation in low energy structure between **1**, **2** and **3** may indicate an alteration of the electronic properties engendered by the inclusion of the extra annulated ring(s) in **1** and **2**.

Simulations of radiolysis involving electron loss or gain

Indirect radiolysis is likely to involve electron transfer and so the effect of adding or removing electrons from various BTP and BATP molecules was considered in order to establish any major difference between the acyclic and aromatic-substituted BATPs. To investigate the effect of electron loss or gain, calculations were first carried out on the four fragments of ligands shown in Fig. 12. Geometry optimisations were carried out on these fragments in their neutral state and also following the gain or loss of one electron. Particular attention was paid to changes in internal bond lengths in the heterocycles and effective ring charges. Effective ring charges and N–N bond lengths for electron removal and addition from/to the four fragments are described in Table 6.

Table 5 The structures with the lowest relative energies for the diprotonated BATP molecules

		(ΔE/kJ mol^{-1})[a]		
Configuration	Atoms protonated	**1**	**2**	**3**
cc	N(11), N(31)	0.00	43.01	0.00
ct	N(11), N(36)	40.50	18.07	−0.63
cc	N(11), N(36)	13.09	0.00	−0.63
ct	N(11), N(31)	29.06	45.93	13.72

[a] Energy relative to the lowest energy configuration.

For each molecule, the partial charges are given for the neutral molecule, the radical cation and anion. In the case of electron addition to fragment C from **1**, it is clear from the effective ring charges that 69% of the electron is localised onto the triazine ring with only 31% on the adjacent saturated ring. A concomitant increase of the N–N bond length is observed to 1.391 Å, indicating possible degradation *via* N–N bond breaking although such an increase is also found in fragments A and B. The magnitude of the increase in N–N bond length (to 1.366 Å) is however significantly less in fragment D from **2**, thus indicating some protection from this mechanism of decomposition is effected by the inclusion of extra annulated rings. However the distribution of the extra electron is similar in fragment D to that found in fragment C with −0.65, −0.26 and −0.09 in the triazine, saturated and aromatic rings, respectively.

Removal of an electron promotes a shortening of the N–N bond and lengthening of the adjacent C–N bonds, suggesting that N_2 expulsion may occur on decomposition.

It is well known that radical cations formed from the 1,2,4-triazines decompose with the formation of dinitrogen, a nitrile and an alkyne.[17] However, while this phenomenon is pronounced in fragments A, B and C, with dimensions of 1.231, 1.239 and 1.240 Å, the bond length in fragment D has decreased less, to 1.257 Å. In fragments A and B, the electron is located on the triazine ring with ring charges of 1.0 and 0.80, respectively. For C however the extra charge is distributed 0.45 to the triazine ring and 0.55 to the saturated ring and substituents. A most interesting result is obtained for fragment D, where the extra charge is distributed 0.06 to the triazine,

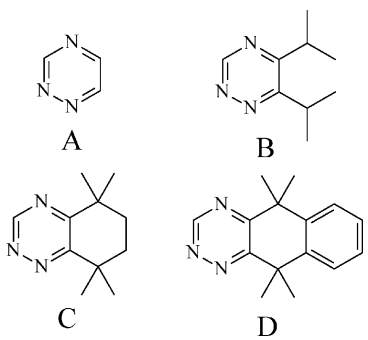

Fig. 12 The four fragments investigated for electron loss and gain. Fragment A is taken from **3**, B from **7**, C from **1**, and D from **2**.

Table 6 Properties of the four fragments (Fig. 10) after addition or removal of an electron

			Charge on nitrogen atoms			Ring charge[a]		
Fragment	Charge	N–N bond length/Å	N(11)	N(13)	N(16)	1	2	3
A	0	1.320	−0.17	−0.26	−0.14	0.0	—	—
	−1	1.397	−0.30	−0.41	−0.31	−1.0	—	—
	1	1.231	0.02	−0.11	0.06	1.0	—	—
B	0	1.321	−0.20	−0.27	−0.14	−0.14	—	—
	−1	1.387	−0.31	−0.40	−0.29	−0.71	—	—
	1	1.239	−0.04	−0.15	0.03	0.80	—	—
C	0	1.316	−0.19	−0.27	−0.15	−0.14	0.14	—
	−1	1.391	−0.30	−0.41	−0.30	−0.69	−0.31	—
	1	1.240	−0.04	−0.15	0.01	0.45	0.55	—
D	0	1.313	−0.19	−0.28	−0.16	−0.17	0.13	0.04
	−1	1.366	−0.28	−0.39	−0.29	−0.65	−0.26	−0.09
	1	1.257	−0.15	−0.26	−0.13	0.06	0.30	0.64

[a] Ring 1 is the triazine, ring 2 is the fused aliphatic ring when present and ring 3 is the fused aromatic ring when present. For atoms shared by rings, their charge is halved and counted in each ring.

0.30 to the saturated ring and 0.64 to the aromatic ring. Thus it could be argued that the triazine ring in fragment D is more stable to electron withdrawal than in the other fragments.

The calculations were repeated for **2** and **3** with two electrons added or removed and the results are shown in Table 7. With two electrons added most of the additional charge (−0.84) is concentrated on the triazine ring in **3** but in **2** this is distributed to some extent in the other rings so that ring charges in the triazine, saturated and aromatic rings, are −0.47, −0.31 and −0.13, respectively. The results for two-electron loss are particularly interesting. For **3** the positive charge is distributed equally on the outer aromatic triazine rings 0.68 and the inner pyridine ring 0.64, but in **2** the majority of the charge is found on the aromatic ring (0.65) while the charge on the triazine ring remains negative at −0.09. This result strongly indicates that direct radiolysis, which probably involves electron loss, in **2** has been averted by the incorporation of extra annulated aromatic rings.

Frontier orbitals and Walsh diagram

The differences in electronic properties of **2** from the other BATPs or BTPs exemplified by **3** are illustrated by the frontier orbitals in the Walsh diagram in Fig. 13. The molecular orbitals of **3** and **2** were calculated using the *cc* conformation, which is to be found in metal complexes. There were, however, only marginal differences between the orbitals calculated from the *cc* and *tt* conformations. The three HOMO and LUMO orbitals shown in this figure for **3** are also typical of those observed for **4**, **5** and **1**, both in the energy differences and the coefficients of the molecular orbitals. However, as can be seen from Fig. 11, while the three LUMOs shown are equivalent, the HOMOs are significantly different. The HOMO in **2** itself is identical to that in **3**, the HOMO-1 and HOMO-2 are degenerate π-orbitals concentrated on the outer rings as indeed are the HOMO-3 and HOMO-4. However, the HOMO-5 and HOMO-6 are similar to the HOMO-1 and HOMO-2 of the **2** and **3**. These orbitals have some σ-contribution from the central nitrogen atom. Hence these four orbitals from HOMO-1 to HOMO-4 inclusive are unique to **2** and demonstrate how the inclusion of the aromatic rings in **2** has altered the electronic properties of the molecule that is reflected in its greater resistance to radiolysis and hydrolysis compared to the other molecules.

Conclusions

Annulated BATP molecules have improved resistance with respect to chemical attack in acid media when compared with

Table 7 Properties of **3** and **2** after addition or removal of two electrons

			Charge on nitrogen atoms				Ring charges			
Molecule	Charge	N–N distance	N(11)	N(13)	N(16)	N(21)	Py	Triazine	Saturated	Aromatic
3	0	1.297	−0.19	−0.21	−0.16	−0.22	0.14	−0.07	—	—
	−2	1.314	−0.21	−0.31	0.27	−0.29	−0.32	−0.84	—	—
	+2	1.224	0.03	−0.10	0.05	−0.20	0.64	0.68	—	—
2	0	1.303	−0.21	−0.25	−0.18	−0.23	0.10	−0.17	0.05	0.08
	−2	1.325	−0.24	−0.35	−0.29	−0.28	−0.29	−0.47	−0.31	−0.13
	+2	1.256	−0.17	−0.25	−0.15	−0.26	0.18	−0.09	0.35	0.65

Ring 1 is the triazine, Ring 2 is the fused aliphatic ring when present and Ring 3 is the fused aromatic ring when present. For atoms shared by rings, their charge is halved and counted in each ring.

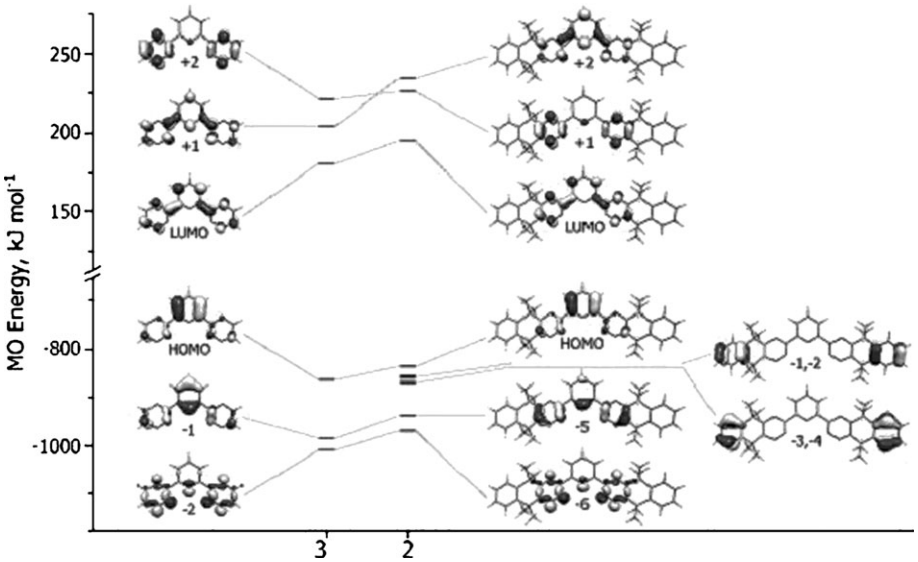

Fig. 13 Walsh diagram for **3** and **2** showing the frontier orbitals.

the reference BTP molecule. Molecule **2** is resistant to both acid hydrolysis and radiolysis. The BATP molecules are able to separate americium(III) from an excess of europium(III) in nitric acid. Minimisation of radiolysis, which probably involves electron transfer, in **2** has been achieved by the incorporation of extra annulated aromatic rings. It has been shown for six coordinate bis-BTP and nine coordinate tris-BTP complexes (respectively by electrochemical and relaxivity experiments) that the annulated side groups in **1** have a greater ability than simple alkyl groups to isolate the central core of the complex.

Acknowledgements

We are grateful for the financial support of the European Union Nuclear Fission Safety Programme Contract FIKW-CT2000-0087—(PARTNEW) and Contract FP6-50508854–(EUROPART). We would also like to thank the EPSRC and the University of Reading for funding of the image plate system.

References

1 G. Choppin, J.-O. Liljenzin and J. Rydberg, *Radiochemistry and nuclear chemistry*, Butterworth-Heinemann, Woburn, 3rd edn, 2002, ch. 21, p. 624.
2 M. Salvatores and A. Zaetta, *Interdiscip. Sci. Rev.*, 1998, **23**, 298.
3 C. Madic, M. J. Hudson, J.-O. Liljenzin, J.-P. Glatz, R. Nannicini, A. Facchini, Z. Kolarik and R. Odoj, *Prog. Nucl. Energy*, 2002, **40**, 523.
4 C. Madic, *Proceedings of the 5th international information exchange meeting on actinide and fission product partitioning and transmutation*, Mol, Belgium, November 25–27, 1998.
5 R. A. Jameson, G. P. Lawreence and C. D. Bowman, *Nucl. Instrum. Methods Phys. Res., Sect. B*, 1992, **68**, 474.
6 S. Andriamonje, F. Carminati, P. Cennini, C. Gelès, I. Goulas, Y. Kadi, R. Klapisch, J. P. Revol, C. Roche, C. Rubbia, J. A. Rubio, F. Saldaña, A. Angelopoulos, A. Apostolakis, K. Sakelariou, L. Sakelliou, G. Zarris, P. Kokkas, P. Pavlopoulos, H. Arnould, C. A. Bompas, R. Del Moral, V. Lacoste, M. Macri, F. Attale, E. Belle, A. Goirni, D. Heuer, J. M. Loiseaux, O. Mépaln, H. Nifenecker, F. Schussler, J. B. Viano, R. Fernández, E. González, J. Aleixandre, J. Bueno, E. Cerro, O. González, J. Tamarit, S. Díez, A. Pérez-Navarro, M. Embid, J. Gálvez, C. López, E. Pérez, M. Poza, S. Vieira, A. Abánades, J. García, M. Perlado, M. Hussonnois, C. Le. Naour, D. Trubert, F. Casagrande, C. Eleftheriadis, G. Kittis, I. Papadopoulos, A. Tzima, V. Vlachoudis and S. Buono, CP447, Nuclear fission and fusion-product spectroscopy: second international workshop, *AIP Conf. Proc.*, ed. G. Fioni, 1998, **447**, 26.
7 Z. Kolarik, U. Mullich and F. Gassner, *Solvent Extr. Ion Exch.*, 1999, **17**, 1155.
8 C. Hill, D. Guillaneux, X. Hérès, N. Boubals and L. Ramain, *Atalante 2000*, Avignon, 2000.
9 K. L. Nash, *Solvent Extr. Ion Exch.*, 1993, **11**, 729.
10 M. G. B. Drew, M. R. S. J. Foreman, N. Huet, M. J. Hudson, C. Hill, C. Madic and T. G. A. Youngs, *Dalton Trans.*, 2003, 1675.
11 N. Boubals, M. G. B. Drew, C. Hill, M. J. Hudson, P. B. Iveson, C. Madic, M. L. Russell and T. G. A. Youngs, *J. Chem. Soc., Dalton Trans.*, 2002, 55.
12 Y. Fukuda, A. Nakao and K. Hayashi, *J. Chem. Soc., Dalton Trans.*, 2002, 527.
13 M. G. B. Drew, M. R. S. Foreman, M. J. Hudson and K. F. Kennedy, *Inorg. Chim. Acta*, 2004, **357**, 4102.
14 C. Hill, D. Guillaneux, L. Berthon and C. Madic, *J. Nucl. Sci. Technol.*, 2002, (Sup. 3), 309.
15 M. J. Hudson, M. G. B. Drew, D. Guillaneux, M. L. Russell, P. B. Iveson and C. Madic, *Inorg. Chem. Commun.*, 2001, **4**, 12.
16 S. Colette, B. Amekraz, C. Madic, L. Berthon, G. Cote and C. Moulin, *Inorg. Chem.*, 2003, **42**, 2215.
17 S. Colette, B. Amekraz, C. Madic, L. Berthon, G. Cote and C. Moulin, *Inorg. Chem.*, 2004, **43**, 6745.
18 M. G. B. Drew, M. J. Hudson, P. B. Iveson, C. M. Madic, J.-O. Liljenzin, L. Spjuth, P.-Y. Cordier, A. Enarsson and C. Hill, *J. Chem. Soc., Dalton Trans.*, 2000, 821.
19 M. J. Hudson, *Czech. J. Phys.*, 2003, **53**, A305.
20 B. J. Mincher, R. E. Arbon, W. B. Knighton and D. H. Meikrantz, *Appl. Radiat. Isot.*, 1994, **45**, 879.
21 B. J. Mincher, R. C. Curry and R. Brey, *Environ. Sci. Technol.*, 2000, **34**, 3452.
22 B. J. Mincher, R. Brey, R. G. Rodriguez, S. Prostupa and A. Ruhter, *Radiat. Phys. Chem.*, 2002, **65**, 461.
23 A. R. Kazanjian, F. J. Miner, A. K. Brown, P. G. Hagan and J. W. Berry, *Trans. Faraday Soc.*, 1970, **66**, 2192.
24 H. Suzuki and T. Mori, *J. Chem. Soc., Perkin Trans. 1*, 1995, 291.
25 A. J. Swallow, *Radiation chemistry of organic compounds*, Pergamon Press Ltd, Oxford, 1960.
26 M. Burton and W. N. Patrick, *J. Phys. Chem.*, 1952, **56**, 560.

27 W. Batey, in *Science and practice of liquid–liquid extraction*, ed. J. D. Thornton, Clarendon Press, Oxford, 1992, vol. 2, p. 139.
28 B. Lambert, V. Jacques, A. Shivanyuk, S. E. Matthews, A. Tunayr, M. Baaden, G. Wipff, V. Böhmer and J. F. Desreux, *Inorg. Chem.*, 2000, **39**, 2033.
29 F. H. Case, *J. Heterocycl. Chem.*, 1971, **8**, 1043.
30 P. Jones, G. B. Villeneuve, C. Fei, J. deMarte, A. J. Haggarty, K. T. Nwe, D. A. Martin, A. M. Lebuis, J. M. Finkelstein, B. J. Gour-Salin, T. H. Chan and B. R. Leyland-Jones, *J. Med. Chem.*, 1998, **41**, 3062.
31 W. J. G. M. Peijneburg and H. M. Buck, *Tetrahedron*, 1998, **44**, 4927.
32 M. R. S. Foreman, M. J. Hudson, M. G. B. Drew, C. Hill and C. Madic, *Dalton Trans.*, 2006, 1645.
33 M. J. Hudson, M. R. S. J. Foreman, C. Hill, N. Huet and C. Madic, *Solvent Extr. Ion Exch.*, 2003, **21**, 637.
34 E. J. Baerends, A. Berces, C. Bo, P. M. Boerrigter, L. Cavallo, L. Deng, R. M. Dickson, D. E. Ellis, L. Fan, T. H. Fisher,C. Fonseca-Guerra, S. J. A. van Gisbergen, J. A. Groeneveld, O. V. Gritsenko, F. E. Harris, D. van Hoek, P. H. Jacobson, G. van Kessel, F. Kootstra, E. van Lenthe, V. E. Osinga, P. H. T. Philipson, D. Post, C. C. Pye, W. Ravenek, P. Ros, P. R. T. Schipper, G. Schreckenback, J. G. Snijders, M. Sola, D. Swerhone, G. te Velde, P. Vernooijs L. Versluis, O. Visser, E. van Wezenbeek, G. Wiesenekker, S. K. Wolff, T. Woo and T. Ziegler, *ADF2000 program*, SCM Inc., Vrije Universiteit, Theoretical Chemistry, Amsterdam, The Netherlands, 2000.
35 A. Klamt, *J. Phys. Chem.*, 1995, **99**, 2224.
36 W. Kabsch, *J. Appl. Crystallogr.*, 1988, **21**, 916.
37 SHELX86: G. M. Sheldrick, *Acta Crystallogr., Sect. A: Found. Crystallogr.*, 1990, **A46**, 467.
38 N. Walker and D. Stuart, *Acta Crystallogr., Sect. A: Found. Crystallogr.*, 1983, **A39**, 158.
39 G. M. Sheldrick, *SHELXL-97, Program for refinement of crystal structures*, University of Göttingen, Germany, 1997.
40 W. R. Robinson, *J. Chem. Educ.*, 1985, **62**, 1001.
41 M. Nilsson, S. Andersson, C. Ekberg, M. R. S. Foreman, M. J. Hudson and G. Skarnemark, *Radiochim. Acta*, 2006, **94**, 103.
42 M. G. B. Drew, M. R. StJ. Foreman, A. Geist, M. J. Hudson, F. Marken, V. Norman and M. Weigl, *Polyhedron*, 2006, **25**, 888.
43 M. G. B. Drew, M. J. Hudson, P. B. Iveson, C. Madic and M. J. Russell, *Inorg. Chem. Commun.*, 2000, **3**, 462.
44 A. N. Landgren and J. O. Liljenzin, *Solvent Extr. Ion Exch.*, 1999, **17**, 1387.
45 E. P. Horwitz, C. A. A. Bloomquist, L. J. Sauro and D. J. Henderson, *J. Inorg. Nucl. Chem.*, 1966, **28**, 2313.
46 *Relaxometry of water–metal ion interactions, advances in inorganic chemistry*, ed. R. van Eldik and I. Bertini, Elsevier, Amsterdam, 2005, vol. 57.
47 *The chemistry of contrast agents in medical magnetic resonance imaging*, ed. A. E. Merbach and E. Toth, Wiley, Chichester, 2001.
48 B. Lambert, V. Jacques, A. Shivanyuk, S. E. Matthews, A. Tunayar, M. Baaden, G. Wipff, V. Böhmer and J. F. Desreux, *Inorg. Chem.*, 2000, **39**, 2033.
49 G. B. Deacon, B. Gortler, P. C. Junk, E. Lork, R. Mews, J. Petersen and B. Zemva, *J. Chem. Soc., Dalton Trans.*, 1998, 3887.